Annals of Nuclear Medicine Vol. 13, No. 4, 235–239, 1999

Pharmacokinetic analysis of ^{123}I-labeled medium chain fatty acid as a radiopharmaceutical for hepatic function based on beta-oxidation

Norio YAMAMURA,* Yasuhiro MAGATA,** Fumiyoshi YAMASHITA,***
Mitsuru HASHIDA*** and Hideo SAJI*

*Department of Patho-Functional Bioanalysis, Graduate School of Pharmaceutical Sciences,
**Department of Nuclear Medicine, Graduate School of Medicine,
***Department of Drug Delivery Research, Graduate School of Pharmaceutical Sciences, Kyoto University

Beta-oxidation is the most important pathway to provide energy for the liver. Our recent findings indicated that radiolabeled medium chain fatty acid analogs could be used as radiopharmaceuticals in the liver, allowing us to monitor alterations in energy metabolism on the cellular level. In the present study, pharmacokinetical analysis of a radioiodinated medium chain fatty acid analog, *p*-[^{123}I]iodophenylenanthic acid ([^{123}I]IPEA), was carried out in normal and hepatitis model rats to investigate the index for the measurement of beta-oxidation activity in hepatocytes. The rate constant for metabolism of [^{123}I]IPEA in the liver showed a strong correlation with the ATP level, which was determined as an indicator of beta-oxidation activity in hepatocytes. The radioactivity profile in the liver after [^{123}I]IPEA administration provided important information regarding hepatic viability, and the metabolic rate constant of [^{123}I]IPEA calculated by a pharmacokinetic method was a useful criterion for hepatic diagnosis based on hepatic cellular energy metabolism.

Key words: medium chain fatty acid, beta-oxidation, pharmacokinetic analysis, hepatic function, SPECT

INTRODUCTION

THE DEVELOPMENT of an *in vivo* method for quantitative and regional assessment of hepatic viability is an important goal of clinical nuclear medicine. For this purpose, we recently developed *p*-[^{123}I]iodophenylenanthic acid ([^{123}I]IPEA) as a radiopharmaceutical for use in single photon emission computed tomography (SPECT) (Fig. 1).[1] [^{123}I]IPEA showed high initial uptake in the liver immediately after the injection. [^{123}I]IPEA incorporated into the liver was metabolized via beta-oxidation, and its radiometabolites were rapidly eliminated from the liver into the urine. In addition, the rate of elimination of radioactivity from the liver was significantly delayed in hepatitis model rats compared with that in normal rats. Thus, in the present study, the hepatic time-activity curves obtained by dynamic scanning with a SPECT instrument were analyzed by a pharmacokinetic method in normal and hepatitis model rats, and some parameters were evaluated as the criteria for determining liver function.

Received February 18, 1999, revision accepted April 13, 1999.

For reprint contact: Hideo Saji, Ph.D., Department of Patho-Functional Bioanalysis, Graduate School of Pharmaceutical Sciences, Kyoto University, Yoshida Shimoadachi-cho, Sakyo-ku, Kyoto 606–8501, JAPAN.

MATERIALS AND METHODS

Materials

Sodium [^{125}I]iodide was purchased from Daiichi Pure Chemical Co. Ltd., Chiba, Japan. Ammonium [^{123}I]iodide was kindly provided by Nihon Medi-Physics Co., Hyogo, Japan. All chemicals were of reagent grade and were used as received.

Synthesis of Radioiodinated IPEA

IPEA was synthesized by iodination of 7-phenylheptanoic acid which was synthesized by Friedel-Crafts reaction from benzene and pimelic acid followed by reduction. Details of the synthetic procedure will be published

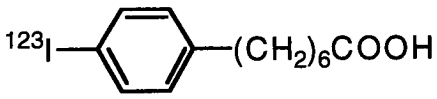

Fig. 1 Chemical structure of [^{123}I]IPEA.

elsewhere. [^{123}I]IPEA and [^{125}I]IPEA were prepared by the ^{127}I-^{123}I or ^{127}I-^{125}I exchange reaction with non-radioactive IPEA as a precursor. The radiochemical purity of each radioiodinated IPEA was more than 96% as determined by high performance liquid chromatography (HPLC) on a reverse-phase column (Cosmosil 5C_{18}-AR-300, 250 mm × 10 mm, Nacalai Tesque, Co., Ltd., Kyoto) with a mobile phase of acetonitrile/water (70/30, v/v) at 30°C (Rt. = 32 min).

Animals

Animal experiments were conducted in accordance with our institutional guidelines and were approved by the Kyoto University Animal Care Committee.

Male Wistar rats (200–250 g) were housed for 1 week under a 12-h light/12-h dark cycle and had free access to food and water. Hepatitis model rats were generated by administration of carbon tetrachloride (CCl_4).[2] Briefly, rats were orally administered 30% CCl_4 (0.5–1.5 m*l* CCl_4/kg) in olive oil (v/v) after a 6-h fast. After fasting for a further 2 h, the animals were fed *ad libitum*.

Metabolite Analysis

Four normal rats anesthetized with pentobarbital were administered 74 kBq of [^{125}I]IPEA via the tail vein. At 20 min post-injection, the rats were sacrificed by decapitation, and the liver was excised immediately. The total lipids in the liver samples were extracted with chloroform/methanol/water (4/2/2) as reported by Forch et al.[3] The organic layer and water-soluble layer were separated, and radioactivity in each was quantified. Then the metabolites in the each layer were analyzed by TLC (reverse-phase TLC plate LKC_{18}F, Whatman International Ltd., Kent, U.K.) developed with acetonitrile/water/acetate (7/3/0.01).

Dynamic Scanning of [^{123}I]IPEA

Imaging studies were performed in 12 rats with a SPECT instrument (SPECT2000H-40, Hitachi Medical Co., Japan). Normal rats and those treated with different doses of CCl_4 were anesthetized with pentobarbital (50 mg/kg i.p.). Dynamic planar scanning (20 sec × 30 frames, 1 min × 10 frames, 2 min × 20 frames) was initiated at the time of [^{123}I]IPEA (18 MBq) injection via the tail vein. Regions of interest (ROI) were chosen on the upper half of the liver images to eliminate the influence of radioactivity from the kidneys, and the time-activity curves were obtained after decay correction.

After scanning, liver samples of about 100 mg were excised from each rat, and the ATP concentration in the liver was measured according to the procedure reported by Sellevold et al. with minor modifications.[4] Briefly, the liver sample was immediately frozen and powdered in liquid nitrogen. Then the ATP in the powdered liver was extracted with 3 m*l* of perchloric acid (0.42 M). After precipitation of proteins and neutralization with potassium hydroxide, ATP was quantified by HPLC on a reverse-phase column (Cosmosil 5C_{18}-AR-300, 150 mm × 4.6 mm, Nacalai Tesque, Co., Ltd., Kyoto) with a mobile phase containing potassium dihydrogen phosphate 215 mM, tetrabutylammonium hydrogen sulfate 2.3 mM, acetonitrile 10% and potassium hydroxide to adjust the pH to 6.0. The flow rate was maintained at 1.0 m*l*/min, and the spectrophotometer was set at 254 nm.

The 12 rats used in this study were divided into 3 groups according to the ATP concentration in the liver as follows: severe injury group, ATP levels of less than 80 μmol/100 g wet liver; moderate injury group, from 80 to 110 μmol/100 g wet liver; and normal group more than 110 μmol/100 g wet liver. Each of these 3 groups consisted of 4 rats.

Data Analysis (Pharmacokinetic Model)

Pharmacokinetic models were constructed based on the following assumptions: (i) [^{123}I]IPEA in the blood was transported into hepatocytes monoexponentially; (ii) [^{123}I]IPEA in the hepatocytes was metabolized by one-way metabolism; (iii) the radiometabolites in the hepatocytes were eliminated from the liver only into blood; and

Table 1 Symbols used in the models

Symbol	Description
X	[^{123}I]IPEA in blood compartment
k_a	Transport rate constant of [^{123}I]IPEA from blood to liver
k_e	Rate constant of elimination of [^{123}I]IPEA by the other organs
X_1	Unchanged [^{123}I]IPEA in liver compartment
X_2	Radiometabolites in liver compartment
$A \cdot e^{-k_1 \cdot t}$	Transport rate of [^{123}I]IPEA from blood to liver
k_2	Transport rate constant of unchanged [^{123}I]IPEA from liver
k_3	Metabolic rate constant in the liver
k_4	Transport rate constant of radiometabolites from liver

Table 2 Mass balance for each compartment in the pharmacokinetic models shown in Figure 2

$\frac{dX}{dt} = -(k_a + k_e) \cdot X$	$X_{t=0} = X_0$
$\frac{dX_1}{dt} = A \cdot e^{-k_1 \cdot t} - (k_2 + k_3) \cdot X_1$	$X_{1,t=0} = 0$
$\frac{dX_2}{dt} = k_3 \cdot X_1 - k_4 \cdot X_2$	$X_{2,t=0} = 0$

Model 1

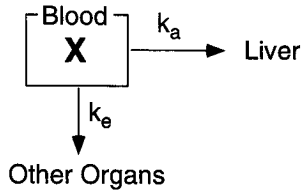

Model 2

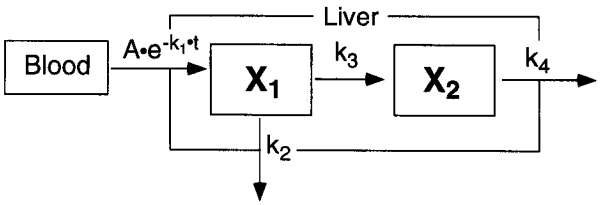

Fig. 2 Pharmacokinetic model used for the analysis of radioactivity profiles following intravenous injection of [^{123}I]IPEA to rats.

Table 3 Pharmacokinetic parameters of [^{123}I]IPEA in rats

	Normal	Moderate injury	Severe injury
A	416.0	395.1	310.9
k_1	3.931	3.811	2.984
k_2	0.0728	0.0461	0.0339
k_3	0.0754	0.0610	0.0502
k_4	0.0042	0.0018	0.0013

(iv) the radiometabolites in blood were not re-accumulated in hepatocytes.

Two pharmacokinetic models are depicted schematically in Figure 2. Symbols and the mass-balance equation are given in Tables 1 and 2, respectively. Model 1 represents clearance of [^{123}I]IPEA from the blood of whole body. Model 2 represents hepatic uptake, metabolism and excretion. The constants k_a and k_e are the rate constants for liver uptake and elimination by the other organs, respectively. Eq. (1) and (2) were obtained from the mass-balance equation shown in Table 2, and Eq. (2) indicated that [^{123}I]IPEA in the blood was transported into hepatocytes monoexponentially. Thus, when $k_a \cdot X$ and $k_a + k_e$ were replaced by A and k_1, respectively, Eq (2) was simplified by $A \cdot e^{-k_1 \cdot t}$ as the input function of [^{123}I]IPEA to the liver.

$$X = X_0 \cdot e^{-(k_a + k_e) \cdot t} \tag{1}$$

$$k_a X = k_a X_0 \cdot e^{-(k_a + k_e) \cdot t} = A \cdot e^{-k_1 \cdot t} \tag{2}$$

The following first-order constants were used in Model 2 (Fig. 2): k_2 for elimination of intact [^{123}I]IPEA from hepatocytes; k_3 for metabolism of [^{123}I]IPEA in hepatocytes; and k_4 for elimination of radiometabolites from hepatocytes. Solving the differential equations for Model 2 (Table 2) yields:

$$X_1 = \frac{1}{k_1 - (k_2 + k_3)} \cdot (-A \cdot e^{-k_1 \cdot t} + A \cdot e^{-(k_2 + k_3) \cdot t}) \tag{3}$$

$$X_2 = \frac{-k_3}{\{k_1 - (k_2 + k_3)\}(k_4 - k_1)} \cdot A \cdot e^{-k_1 \cdot t} + \frac{k_3}{\{k_1 - (k_2 + k_3)\}\{k_4 - (k_2 + k_3)\}} \cdot A \cdot e^{-(k_2 + k_3) \cdot t} + \frac{k_3}{\{k_4 - (k_2 + k_3)\}(k_4 - k_1)} \cdot A \cdot e^{-k_4 \cdot t} \tag{4}$$

$$X_1 + X_2 = \frac{k_1 - (k_3 + k_4)}{\{k_1 - (k_2 + k_3)\}(k_4 - k_1)} \cdot A \cdot e^{-k_1 \cdot t} + \frac{k_4 - k_2}{\{k_1 - (k_2 + k_3)\}\{(k_4 - (k_2 + k_3)\}} \cdot A \cdot e^{-(k_2 + k_3) \cdot t} + \frac{k_3}{\{k_4 - (k_2 + k_3)\}(k_4 - k_1)} \cdot A \cdot e^{-k_4 \cdot t} \tag{5}$$

Since it was impossible to distinguish radioactivity from intact [^{123}I]IPEA and that from radiometabolites in the hepatocytes by external imaging, the information obtained from the hepatic images on radioactivity represents the sum of them ($X_1 + X_2$).

The equation for the amount of radioactivity in the liver ($X_1 + X_2$) (Eq. 5) was fitted to the radioactivity profiles obtained by dynamic scanning of [^{123}I]IPEA by the non-linear least-squares method (MULTI),[5] and constants k_1, k_2, k_3, k_4 and A were determined.

RESULTS AND DISCUSSION

Figure 3 shows the mean time-activity profiles of the livers obtained by dynamic scanning of each group. These results are shown by the relative radioactivity in the liver in order to evaluate the clearance rate. The normal group showed a higher initial uptake and faster clearance in the liver than the CCl_4-treated group. Although about 44% of the maximum radioactivity uptake in the liver remained in the normal rats at 60 min after injection, this might be the result of the slower elimination from the liver of the radiometabolite rather than its production through beta-oxidation and/or of the relatively high background seen in the planar image. All of these time-activity profiles showed two phase clearance. Although the second phase clearance was not clearly different among these groups, the first phase clearance was delayed depending on the degree of injury due to CCl_4. That is, at each clearance point in the severe injury group and after 5 min of moderate injury the portion of radioactivity remaining in the liver was significantly higher than that in the normal group.

Administration of CCl_4 causes peroxidation of fat, which causes the collapse of systems enclosed by membranes including mitochondria.[6,7] The enzymes involved in beta-oxidation are located in the mitochondrial matrix.[8]

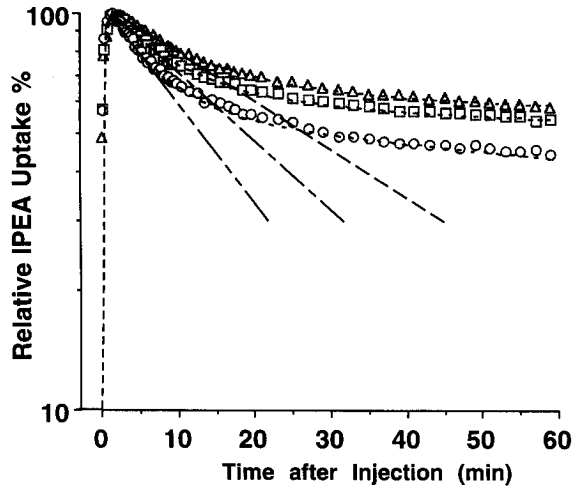

Fig. 3 Time-activity curves in the liver following [^{123}I]IPEA administration. The rats used in the imaging study were divided in 3 groups by ATP level in the liver. The equation to determine the amount of radioactivity in ROI on the liver was fitted to mean radioactivity profiles by MULTI. The elimination of radioactivity from the liver was delayed in the severe injury group (△) and moderate injury group (□) compared with the normal group (○).

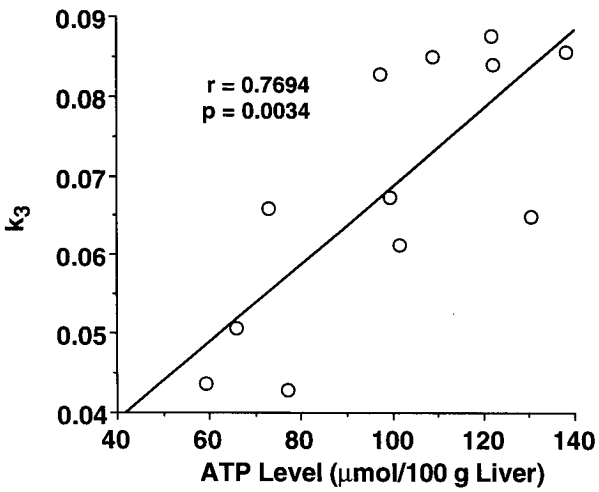

Fig. 4 Correlation between [^{123}I]IPEA metabolic rate constant k_3 and ATP level in the liver. The equation to determine the amount of radioactivity in the ROI on the liver was fitted to the radioactivity profile of each of 12 rats individually by MULTI. A good correlation (r = 0.7694, p = 0.0034) was observed between both parameters.

Therefore, the model animals used in the present study were expected to suffer damage to the beta-oxidation system, although other injuries also seemed to have occurred. Therefore, the delay in radioactivity clearance observed in the present study may have been responsible for the lack of normal beta-oxidation.

The models shown in Figure 2 were therefore established and the time-activity profiles were fitted based on these models by using the MULTI program. The fitted values for parameters in each group are shown in Table 3.

Table 4 Metabolite analysis in liver

	Experimental	Calculated
$\frac{X_2}{X_1 + X_2} \times 100$	85.5 ± 0.2	89.4

Metabolite analysis showed that 85.5% of radioactivity in the normal rat liver was derived from radiometabolites of [^{123}I]IPEA. This percentage matched the calculated $\frac{X_2}{X_1 + X_2} \times 100$ value for normal rats based on Eq. 5 (Table 4). Therefore, since the present pharmacokinetic model was considered appropriate, it was also applied to experimental data analyses for hepatitis model rats.

For further investigation on the index of beta-oxidation activity in hepatocytes, the time-radioactivity profile of each animal was fitted individually. The rate constant k_3 was considered to be related to beta-oxidation in hepatocytes based on Model 2. On the other hand, since beta-oxidation is the main pathway responsible for production of ATP in the hepatocytes,[9,10] the level of ATP in the liver was regarded as an indicator of the beta-oxidation activity in hepatocytes. Therefore, the relationship between the first-order constant k_3 for the metabolic rate of [^{123}I]IPEA in hepatocytes and the ATP concentration in the liver was evaluated as shown in Figure 4. There was a good correlation between k_3 and the ATP level (r = 0.769). This indicated that k_3 is a potentially useful criterion which allows determination of the beta-oxidation activity in hepatocytes externally after [^{123}I]IPEA administration.

The metabolic rate via the beta-oxidation in the liver might be influenced by the anesthetic. But in order to eliminate the effect of the anesthetic, in all experiments in the present study the same anesthetic was used, and further study of the anesthetic may be required to elucidate its effect.

In conclusion, when [^{123}I]IPEA was administered to rats, the degree of injury in hepatocytes due to CCl_4 could be detected as the delay in radioactivity clearance from the liver. Furthermore, pharmacokinetic analysis indicated that the rate constant k_3 for metabolism of [^{123}I]IPEA could be used to quantify hepatocyte viability based on beta-oxidation activity.

REFERENCES

1. Yamamura N, Magata Y, Iida Y, Kitano H, Konishi J, Saji H. Evaluation of radioiodinated medium chain fatty acids as new diagnostic agents for regional liver function. *KAKU IGAKU (Jpn J Nucl Med)* 35: 595, 1998.
2. Hjelle JJ, Grubbs JH, Beer DG, Petersen DR. Time course of the carbon tetrachloride-induced decrease in mitochondrial aldehyde dehydrogenase activity. *Toxicol Appl Pharmacol* 67: 159–165, 1983.
3. Forch J, Less M, Sloane-Stanley GH. A simple method for

the isolation and purification of total lipids from animal tissues. *J Biol Chem* 226: 497–509, 1957.
4. Sellevold OFM, Jynge P, Aarstad K. High performance liquid chromatography: a rapid isocratic method for determination of creatine compounds and adenine nucleotides in myocardial tissue. *J Mol Cell Cardiol* 18: 517–527, 1986.
5. Yamaoka K, Tanigawara Y, Nakagawa T, Uno T. A pharmacokinetic analysis program (MULTI) for microcomputer. *J Pharmacobiodyn* 4: 879–885, 1981.
6. Lossow WJ, Chaikoff IL. Carbohydrate sparing of fatty acid oxidation. I. The relation of fatty acid chain length to the degree of sparing. II. The metabolism by which carbohydrate spares the oxidation of palmitic acid. *Arch Biochem Biophys* 57: 23–40, 1955.
7. Cotran RS, Kumer V, Robbins SL. Cellular injury and adaptation. *In*: Robbins Pathologic Basis of Disease. Cotran RS, Kumer V, Robbins SL (eds.), Philadelphia: W.B. Saunders, pp. 1–38, 1989.
8. Bennett MJ. The enzymes of mitochondrial fatty acid oxidation. *Clin Chim Acta* 226: 211–224, 1994.
9. Martin DB. Metabolism and energy mechanisms. *In*: Pathophysiology. Frohlich ED (ed.), Philadelphia: Lippincott, pp. 365–383, 1976.
10. Zakim D. Metabolism of glucose and fatty acids by the liver. *In*: Hepatology. Zakim D, Boyer TD (eds.), Philadelphia: Saunders, pp. 76–109, 1982.